Identification and validation of a novel LncRNA TRG-AS1 that inhibits colorectal cancer proliferation and glycolysis

Lu Li
Zhengzhou Central Hospital Affiliated to Zhengzhou University
Yong Zhang
Zhengzhou Central Hospital Affiliated to Zhengzhou University
Kunkun Li
Zhengzhou Central Hospital Affiliated to Zhengzhou University
Mengxuan Xing
Zhengzhou Central Hospital Affiliated to Zhengzhou University
Xingguo Xiao
Zhengzhou Central Hospital Affiliated to Zhengzhou University
Li Zhang
Zhengzhou Central Hospital Affiliated to Zhengzhou University
Feifei Chu
Zhengzhou Central Hospital Affiliated to Zhengzhou University
Huili Wu (wuhuili660912@zzu.edu.cn)
Zhengzhou Central Hospital Affiliated to Zhengzhou University

Research Article

Keywords: Colorectal cancer, LncRNA TRG-AS1, Proliferation, Glycolysis

Posted Date: May 18th, 2022

DOI: https://doi.org/10.21203/rs.3.rs-1521203/v2

Abstract

Background

Glucose metabolism reprogramming is one of the major hallmarks of malignant tumors and is regulated by long non-coding RNA (LncRNA). However, the role of glycolysis-associated LncRNA in colorectal cancer (CRC) remains largely unknown. In this study, we identified a novel LncRNA TRG-AS1 that inhibits CRC glycolysis and proliferation through comprehensive bioinformatics analysis and experimental validation.

Methods

TRG-AS1 overexpressing stable cell line and silence the target gene cell line were generated. Glucose assay kits and Pyruvate assay kits were utilized to analyze glycolysis. The cell proliferation ability was evaluated by CCK8, Colony formation assays and EdU. Xenograft tumor experiments were performed to assess proliferative capacity. Cell migration and invasion abilities were examined using the Transwell assay.

Results

TRG-AS1 was significantly down-regulated in CRC tumors as revealed by nine independent CRC cohorts, including our own in-house cohort. Clinically, high expression of TRG-AS1 predicts favorable overall survival (OS) and disease-free survival (DFS) in CRC patients, and high level of TRG-AS1 is closely associated with earlier tumor stage. In terms of function, over-expression of TRG-AS1 significantly inhibited CRC aerobic glycolysis, proliferation, metastasis potential and tumor growth, while knockdown of TGR-AS1 dramatically promoted CRC aerobic glycolysis and progression. Data based on bioinformatics analysis suggest that TRG-AS1 may be involved in CRC progression by influencing glycolysis-related molecules, such as SLC2A1, PGK1 and ENO1, etc.

Conclusion

Our study advances the understanding that LncRNA inhibits CRC glycolysis and progression, and provide a promising molecular target for the treatment of CRC.

1. Background

Colorectal cancer (CRC), ranked as the third in terms of cancer-related morbidity and second in terms of cancer-related mortality, is one of the most common malignancies worldwide according to the GLOBOCAN 2020[1]. Numerous studies have demonstrated that several risk factors such as hereditary susceptibility, epigenetic changes, age, sex, obesity, red meat consumption, alcohol, smoking, and

sedentary lifestyle are considered to contribute significantly to colorectal cancer initiation and progression [2–5]. Recently, the incidence of CRC is still on the rise and shows younger trend [6]. CRC pathogenesis is a multifactorial, multistep, complicated biological process which involves the expression of both coding and non-coding genes [7–9]. As CRC is highly heterogeneous and intricate in molecular pathogenesis, the underlying mechanisms of initiation and development remain largely unknown [10]. Therefore, further exploring the molecular mechanism involved in the development of CRC and finding potential biomarker is indispensable for establishing better diagnosis and treatments for CRC.

Long non-coding RNA (lncRNA) belongs to a type of limited coding capacity transcript, which have a length of more than 200 nucleotides [11–14]. A large amount of studies has been identified that lncRNA plays a vital role in the biological functions of cancer, such as initiation, progression, metastasis, and chemotherapy resistance, particularly in CRC [15–19]. It is currently thought that the dysregulation of lncRNAs promoted to malignant progression of cancer at the epigenetic, transcriptional, and post-transcriptional levels [20, 21]. Some lines of evidences indicate that lncRNAs affect the transcriptional and epigenetic regulation of gene expression by acting as decoys for transcription factors, miRNA sponges, RNA interference, scaffolds for ribonucleoprotein complexes, recruiters of chromatin-modifying complexes, transcriptional regulation in cis or trans [22–25]. These findings indicate that lncRNAs may be potential biomarkers for CRC.

Metabolic reprogramming, which is one of the hallmarks of cancer, is one of the key drivers of the cancer initiation and progression [26–28]. Reprogramming of cellular metabolism accelerates the rapid proliferation and long-term maintenance of cells [29, 30]. LncRNAs are able to regulate complex biological processes via diverse mechanisms, particularly in glycolysis, de novo synthesis of lipids, glutamine and mitochondrial metabolism [31, 32]. However, studies on the involvement of lncRNA regulation on glycolysis in CRC have been limited.

In the present study, we obtained LncRNAs related with CRC by bioinformatics analysis from public databases, in which TRG-AS1 was identified because of lower expression and correlated with prognostic features. Subsequently, the expression of TRG-AS1 was validated in paired clinical samples and CRC cell lines. As a tumor suppressor, over-expression of TRG-AS1 significantly inhibited CRC cell proliferation, facilitated cell apoptosis and suppressed glycolysis. Silencing TRG-AS1 remarkably contributed to CRC cell proliferation and glycolysis, curbed cell apoptosis. Collectively, we investigated the functional of the TRG-AS1 in the progression of colorectal cancer for the first time. This study provides a novel perspective in elucidating the mechanism of the occurrence and development of colorectal cancer and searching for potential biomarkers.

2. Methods

2.1 Bioinformatics Analysis

2.1.1 Data collection

The RNA sequencing (RNA-seq) dataset (including FPKM and read count) and clinical data of 622 CRC (including COAD and READ) patients were retrieved from the TCGA Project in UCSC (https://xenabrowser.net/datapages/). Seven independent datasets including GSE15960 (6 patients), GSE9348 (32 patients), GSE8671 (32 patients), GSE37364 (38 patients), GSE33133 (90 patients), GSE21510 (123 patients) and GSE39582 (443 patients) were downloaded from Gene Expression Omnibus (GEO), and gene expression was detected by the GPL570 platform of U133 plus 2 array.

2.1.2 Identify novel differentially expressed LncRNAs

The differential expression analysis was performed by comparing the expression profiles between tumor samples and normal samples for the expression data (read counts) detected by RNA-seq in TCGA, differentially expressed genes (DEGs) were identified using R package EdgeR and Deseq2 [33] with FDR ≤ 0.05 and fold change (FC) ≥ 2 or ≤ 0.5. For subsequent validation, only DEGs with high-expression level (median FRKM expression > 1) were retained, and probes were annotated on the GPL570 platform. For the expression data detected by GPL570 platform, the DEGs were identified using Limma [34] with FDR ≤ 0.05 and FC ≥ 1.2 or $\leq 1/1.2$ in GEO datasets.

2.1.3 Evaluation of the LncRNA related prognostic model

Except for differential expression analysis, $\log_2$ (FPKM + 1) was conducted for other analysis in TCGA. In TCGA and GEO datasets, CRC patients were stratified into two subgroups based on the median level of TRG-AS1 expression. The survival curves (including overall survival and disease-free survival) were estimated using the Kaplan-Meier method, and the log-rank test was utilized to analyze differences in survival time. The p value < 0.05 was considered as statistically significant.

2.1.4 Functional enrichment analysis

Pearson correlation analysis was adopted to estimate expression correlation of TRG-AS1 and the key enzyme of glycolysis. In TCGA, CRC patients were stratified into two subgroups based on the median level of TRG-AS1 expression. Differential expression analysis was used to obtain the gene list associated with TRG-AS1 GO enrichment analysis and GSEA analysis were implemented using ClusterProfiler package based on MsigDB datasets [35].

2.2 Tissue specimens

Participants were recruited from subjects who underwent endoscopy and were pathologically diagnosed with colorectal cancer at Zhengzhou central Hospital Affiliated to Zhengzhou University during the period 2020–2021. Patients were excluded if they were confirmed or highly suspicious for recurrent gastric cancer, secondary malignant disease, received chemotherapy, immunotherapy, or radiotherapy [36]. Finally, 66 patients with complete information were included in this cohort. Detailed clinical characteristics were presented in Table 1. The procedures used in this study adhere to the tenets of the Declaration of Helsinki. With institutional review board approval (Ethical Batch Number:202021), and following informed consent, tumor tissue and paired normal tissue were collected and promptly frozen in a -80°C refrigerator.

Table 1
Detailed clinical characteristics

clinical characteristics		n = 66	%(n = 66)
Age(years)			
	≤ 60	20	30.30%
	> 60	46	69.70%
Gender			
	Male	39	59.09%
	Female	27	40.91%
Tumor volume			
	≤ 5cm^3	21	31.82%
	> 5cm^3	45	68.18%
Depth of invasion			
	T1-T2	6	9.09%
	T3-T4	60	90.91%
Metastasis			
	Yes	35	53.03%
	NO	31	46.97%
TNM stage			
	I + II	29	43.94%
	III + IV	37	56.06%
Serum CEA level			
	≤ 10 ng/ml	51	77.27%
	10 ng/ml	15	22.73%
Grade			
	G1 + G2	46	69.70%
	G3 + G4	20	30.30%
Smoking history			
	Yes	11	16.67%

clinical characteristics		n = 66	%(n = 66)
	NO	55	83.33%
Drinking history			
	Yes	10	15.15%
	NO	56	84.85%

2.3 Cell culture

All colorectal cancer cell lines including NCM460 (RRID:CVCL_0460), HCT8 (RRID:CVCL_2478), HCT116 (RRID:CVCL_0291), HT29 (RRID:CVCL_0320), SW480 (RRID:CVCL_0546), CaCo2 (RRID:CVCL_0025), RKO (RRID:CVCL_HE15) and Lovo (RRID:CVCL_0399) were purchased from Procell Life Science Technology, routinely monitored by PCR to ensure they were mycoplasma free and authenticated by STR profiling. NCM460 and HCT8 cells were cultured in RPMI 1640 medium. HCT116 and HT29 cells were cultured in McCoy's 5A medium. SW480 cells were cultured in IMDM medium. CaCo2 cells were cultured in DMDM medium. All culture media were supplemented with 10% heat-inactivated fetal bovine serum (FBS, Gibco, Carlsbad, CA), 100U/ml penicillin, and 100 mg/ml streptomycin (Beijing Solarbio Science & Technology). All cells were cultured under standard incubator conditions (37°C, 5% CO_2) and passaged at approximately 90% confluence.

2.4 Quantitative Reverse Transcription Polymerase Chain Reaction (qRT-PCR)

Total RNA was extracted from tissues and cells using reagent (Invitrogen, USA) and RNeasy Mini Kit according to the manufacturer's instructions. RNA concentration and purity were measured on the Nanodrop 2000, and the RNA integrity was verified by gel electrophoresis. First-strand cDNA was synthesized from the total RNA using a reverse transcriptional kit (Invitrogen, USA). Quantitative RT-PCR was performed on an Applied Biosciences 7500 Real-Time PCR system following the QuantiTect SYBR Green PCR kit protocols (Qiagen). A list of primer sequences is reported in Table 2. Glyceraldehyde 3-phosphate dehydrogenase (GAPDH) was used for normalization and relative abundance of lncRNA and mRNA. The 2 − ΔΔCTmethod was used to calculate the expression of LncRNA [37].

2.5 Cell Transfection

When 50% confluent, transient transfection of cells were performed using interferin transfection reagent (Polyplus-transfection), according to manufacturer's instructions. The sequences of negative control small interfering RNA (siRNA) and on-target individual siRNAs were described in Table 2 and were synthesized by Shanghai GenePharma. siRNA oligonucleotides were transfected at a final working concentration of 20 nmol and kept at − 20°C. Six hours after transfection, the culture medium was replaced. The knockdown and transfect efficiency of siRNA was determined 48 hours post transfection by qRT–PCR.

Table 2
The primers and siRNAs used in this study.

Human Gene	Sequences (5'- 3')
GAPDH	Forward primer: CCGGGAAACTGTGGCGTGATGG
	Reverse primer: AGGTGGAGGAGTGGGTGTCGCTGTT
LncRNA TRG-AS1	Forward primer: GCCTAGGCTAATGTGTGGCT
	Reverse primer: AGGCAGAAGAGTCGCTTGAC
Si RNA-NC	Sense: UUCUCCGAACGUGUCACGUTT
	Antisense: ACGUGACACGUUCGGAGAATT
Si RNA TRG-AS1#1	Sense: GGACUACAGUGAUAUUGAAGA
	Antisense: UUCAAUAUCACUGUAGUCCAG
Si RNA TRG-AS1#2	Sense: GGUUUAUGUAAUUACUAUAUU
	Antisense: UAUAGUAAUUACAUAAACCAG
Si RNA TRG-AS1#3	Sense: GGUUGAAUGUUCUUUAUAAA
	Antisense: UAAUAAAGAACAUUCAACCCU

2.6 Lentivirus packaging and stable cell lines

Lentiviral vectors that stably overexpressing lncRNA TRG-AS1 (OE-TRG-AS1) and negative control lentiviral vectors (OE-NC) were designed and packaged by Shanghai Jikai Gene Company. HCT116 and SW480 cells were transfected with lentivirus /medium at a ratio of 1:50. Transfection efficiency was confirmed by observing the fluorescence of green fluorescent protein (GFP) carried by the viral vector, whereas lncRNA TRG-AS1 levels were verified by real-time PCR.

2.7 Glucose uptake assay

Cells were collected and re-suspended in distilled water, ultrasonic wave disruption the cells in ice bath with 120W for 7min. The mixture was placed in a boiling water bath for 10min, cooled at room temperature, and then centrifuged after cooling at 8000g for 10min. After add 180μL mix reagent to 20μL supernatant and incubation at 37°C for 15min, the absorbance values at 505 nm were determined.

2.8 Pyruvate assay

Cells were collected and re-suspended in extraction buffer, ultrasonic wave disruption the cells in ice bath with 120W for 7min. The homogenate was left to stand for 30min, centrifuged for 10min at 8000g and the supernatant was removed. Standard solution in the kit was used to prepare the standard curve. The working solution was added to supernatant, which was left for 2min and then added to working solution . Absorbance was measured at a wavelength of 520 nm.

2.9 CCK-8 cell viability assays

Cell counting kit 8 (CCK8) experiment for in vitro proliferation assay were performed using the CCK8 Kit (Sigma-Aldrich) according to the manufacturer's protocol. The transfected cells were seeded into 96-well plates at a density of 2000 cells per well with 6 replicates. The medium was replaced with 100μl fresh complete medium containing 10μl CCK8 solution following a culture of 0, 24, 48 and 72h, respectively. Then, the plates were incubated at 37°C and 5% CO2 for 2h, and the absorbance was measured at a wavelength of 450nm.

2.10 Colony formation assays

1000 cells/well were plated in 6-well plates, and pools of cells were used to assess growth and clonogenic ability. Ten days after plating the cells, clonogenic progenitors were determined and cells in each group were replated for 6 times. Colonies were rinsed twice with ice-cold PBS, fixed with 4% paraformaldehyde for 20 min on ice and washed twice with PBS. After fixed with methanol, cells were stained with 0.1% crystal violet solution 30 min and then the colonies were imaged and counted.

2.11 Ethynyl deoxyuridine (EdU) Staining

Transfected cells were inoculated at a density of 2×10^4/ml per well in 96-black bottom. A total of 6 reduplicate wells were set up for each group. EdU staining using the Click EdU kit (Abbkine, USA) was performed according to protocol. Cells were incubated with basal medium containing 10μM EdU at 37°C for 2h. Subsequently, cells were fixed with 4% paraformaldehyde for 30min followed by washing with 3% BSA and permeabilization with 0.1% Triton X-100. Afterwards the cells were stained with 50μL of fresh reaction cocktail, and the nucleus was stained with 50μL of DAPI, followed by viability determination with a fluorescence microscope (LEICA DFC450C). The EDU-positive cells were counted in five random visual fields from each well and percentages were calculated.

2.12 Cell migration and invasion assays

Transfected cells resuspended in serum-free medium were seeded into the upper chamber of 24-well inserts with or without Matrigel (BD, USA). Then, 600ul of medium supplemented with 20% FBS was added into the lower chamber. After incubation for 24 hours (SW480) or 36 hours (HCT116), non-invading cells in the upper chamber were scraped off. The cells on the bottom surface of the chambers were fixed using 4% paraformaldehyde, and stained with crystal violet solution. Invading cells or migrating cells were photographed and counted under a light microscope (LEICA DFC450C).

2.13 In vivo tumor xenograft experiments

Ten 6-week-old BALB/c male nude mice were used for the tumor xenograft experiment. The cell suspensions of HCT116-OE-NC and OE-TRG-AS1 were inoculated subcutaneously on the upper right forelimb of nude mouse, respectively. The body weight and tumor morphology were recorded. Tumor volume was measured every 3d with a vernier caliper and calculated as $0.5 \times \text{width}^2$ (cm^2) × length (cm).

All experimental procedures have been approved by the Ethics Committee of Zhengzhou Central Hospital Affiliated to Zhengzhou University.

2.14 Statistical Analysis

The data were presented as mean ± standard deviation. Statistical analysis between two groups was performed using the Student's t-test. The expression correlation was determined by Pearson coefficient analysis. The correlation between TRG-AS1 expression and clinicopathological features of CRC patients was evaluated by Chi-square test. The $P < 0.05$ was considered significant. Statistical analysis was performed on SPSS 24.0.

3. Results

3.1 Identify differentially expressed glycolysis-related LncRNAs in CRC and normal tissues

To explore the potential involvement of lncRNAs in colorectal cancer, we analyzed the lncRNA expression analysis across the seven GEO datasets and TCGA dataset. 585 (328 up-regulated and 257 down-regulated lncRNAs) and 6782 (3611 up-regulated and 3171 down-regulated lncRNAs) differentially expressed lncRNAs (DElncRNAs) were identified (Fig. 1A). Interaction diagram based on high confidence, 9 significantly up-regulated and 23 down–regulated lncRNAs were obtained. The change in direction of expression of TCGA is consistent with the GEO datasets, and the intersection is shown in Fig. 1B-C.

To consider whether those DElncRNAs were closely related to the overall survival (OS) and disease-free survival (DFS) of CRC patients in the TCGA and GEO cohort, we performed the univariate Cox regression to identify the prognostic value of the DElncRNAs for OS and DFS. Among the 21 differentially expressed down- regulated DElncRNAs, TRG-AS1 had a significant association with the patient’s survival. The workflow of lncRNA identification was presented in Fig. 1D. Collectively, these results indicated that TRG-AS1 could be a suppressor lncRNA with a potential prognostic capability.

3.2 Confirmation of the differential expression of lncRNA TRG-AS1 in CRC

Based on all of the results described above, the expression and role of TRG-AS1 in CRC has not been well characterized at present. Therefore, we selected TRG-AS1 for further study. Analysis of the human CRC datasets from 8 public cancer databases contained 1498 patients revealed that TRG-AS1 expression level was significantly decreased in CRC samples compared with that in normal colon tissues (Fig. 2A-H). The TGA-AS1 expression was down-regulated by microarray analysis in 6 Hungarian intestinal adenocarcinoma patients compared to paired normal tissues [38]. This phenomenon was validated in a study from the University of Zurich in 32 CRC patients [39]. Additionally, a Singapore study found that TRG-AS1 expression was decreased in CRC patients compared to healthy subjects [40]. This was also revealed by microarray data from 65 independent samples from the Hungarian [41]. The sequencing

results of the 96 samples from the Netherlands were consistent [42]. Results remained generally stable, regardless of different races and regions [43, 44]. We next verified the expression pattern of TRG-AS1 by 66 pairs of clinical samples from our center. Consistently, the expression of TRG-AS1 in tumor tissue was obviously lower compared with the normal colon tissue by qRT-PCR (Fig. 2I). As expected, TRG-AS1 expression was down- regulated in CRC cell lines compared with normal colon epithelium (NCM460) (Fig. 5A). The results suggest that TRG-AS1 was significantly down-regulated in CRC cells and tumor tissue from CRC patients.

3.3 Confirmation of potential prognostic value of lncRNA TRG-AS1 in CRC

High and low TRG-AS1 expression was determined based on the median patient expression level. Kaplan-Meier survival curve revealed that the CRC patients with lower TRG-AS1 expression were associated with poorer OS and DFS (Fig. 3A-D). We further investigated the relationship between TRG-AS1 expression and clinicopathological characteristics in CRC. The TRG-AS1 expression was declined as the tumor stage progressed in TCGA dataset (Fig. 3E). The result was validated in our cohort (Fig. 3I). The TRG-AS1 expression was significantly associated with lymph node and distant metastases in TCGA cohort (Fig. 3F-G). In addition, the Affymetrix GeneChip arrays data of 155 colorectal cancer tissues from 8 different centers were further performed [45]. Specifically, increased TRG-AS1 expression was more prominent in microsatellite instability tumors compared with microsatellite stable tumors(Fig. 3H). Microsatellite status is an important factor in the prognostic predictive value of CRC, and high-microsatellite instability was significantly associated with a favorable prognosis in CRC patients [46]. This suggests that the TRG-AS1 is of high value for the prognosis of CRC patients. Meanwhile, this potentially demonstrates a marked advantage of TRG-AS1 in guiding the clinical therapy of CRC. Next, the correlation between the expression level of LncRNA TRG-AS1 and clinical data was verified through our samples, and we present the results in Table 3. LncRNA TRG-AS1 expression is markedly associated with depth of invasion, metastasis and tumor size in our cohort (Fig. 3J-L). Collectively, these results indicate that lncRNA TRG-AS1 could be a suppressor lncRNA with a potential prognostic capability.

Table 3
The relationship between LncRNA TRG-AS1 expression and clinical characteristics

clinical characteristics	LncRNA TRG-AS1 expression		*P* value
	Low	High	
Age(years)			0.7893
≤ 60	9	11	
> 60	24	22	
Gender			0.8023
Male	19	20	
Female	14	13	
Tumor volume			0.0012
≤ $5cm^3$	4	17	
> $5cm^3$	29	16	
Depth of invasion			0.0244
T1-T2	0	6	
T3-T4	33	27	
Metastasis			0.0001
Yes	30	5	
NO	3	28	
TNM stage			0.0001
I + II	0	29	
III + IV	33	4	
Serum CEA level			0.2396
≤ 10 ng/ml	23	28	
> 10 ng/ml	10	5	
Grade			0.2840
G1 + G2	21	25	
G3 + G4	12	8	
Smoking history			0.5105

clinical characteristics	LncRNA TRG-AS1 expression		*P* value
	Low	High	
Yes	4	7	
NO	29	26	
Drinking history			0.7330
Yes	4	6	
NO	29	27	

3.4 Potential biological functions of lncRNA TRG-AS1 in CRC

We next intended to investigate the biological functions of TRG-AS1 in CRC. 622 CRC patients were divided into two groups depending on the median expression of TRG-AS1 from the TCGA database, and the associated mRNAs were identified by differential expression analysis. To determine the biological and functional significance of the differentially expressed genes, we performed an enrichment analysis of gene ontology (GO) terms and Gene Set Enrichment Analysis (GSEA) using Molecular Signatures Database (MSigDB). The enrichment analysis revealed that the differentially expressed mRNAs were enriched in cell proliferation, glycolysis, immune, and so on (Fig. 4A-B). Furthermore, Pearson correlation test from multiple sets of databases demonstrate a significant inverse correlation between TRG-AS1 expression and key rate-limiting enzymes of glycolysis, including SLC2A1, PGK1 and ENO1 (Fig. 4C-E). These observations suggest that lncRNA TRG-AS1 contributed to cell glycolysis and proliferation.

3.5 LncRNA TRG-AS1 contributes to weakened glycolysis

Next, to ascertain whether TRG-AS1 regulates the biological functions of colorectal cancer cells, the expression of lncRNA TRG-AS1 was down-regulated in HCT116 and SW480 cells (Fig. 5A). LncRNA TRG-AS1 overexpression was carried out. At 48 h after transfection treatment, the expression efficiency was measured by qRT-PCR (Fig. 5B). The bioinformatic analysis revealed TRG-AS1 might be involved in glycolysis of CRC. To investigate the effect of TRG-AS1 on the glycolysis of CRC cells, glucose uptake and pyruvate levels were then detected. The over-expression of lncRNA TRG-AS1 significantly decreased glucose uptake and pyruvate production (Fig. 5C-D).

HCT116 and SW480 cells were transiently transfected three lncRNA TRG-AS1-specific small interfering RNAs (siRNAs) or with an unrelated siRNA (Si-NC). At 48 h after transfection treatment, the expression efficiency was measured by qRT-PCR analysis (Fig. 5E). Then, siRNA1(Si-1) and siRNA3(Si-3) were selected for further experiments. Compared with control group, TRG-AS1 silencing can accelerated the metabolic process, resulting in an increase of glucose uptake, lactate production, and pyruvate consumption (Fig. 5F-G). In accordance, these results showed that LncRNA TRG-AS1 contributes to weakened glycolysis.

3.6 LncRNA TRG-AS1 suppress the proliferation of CRC cells

Glycolysis is well associated with the regulation of cell proliferation [47]. Consequently, the effect of TRG-AS1 on cell proliferation was further investigated. Compared with the OE-NC group, the overexpression of TRG-AS1 inhibited the proliferation of HCT116 and SW480 cells as measured by the CCK8 assay, colony formation and EdU in vitro experiment (Fig. 6A-C). Tumor xenograft experiment was carried out to evaluate the effect of TRG-AS1 on the tumorigenic ability of HCT116 cell. The results showed that overexpression of TRG-AS1 effectively suppressed the tumorigenicity, reduced the tumor size and weight comparing with control cells (Fig. 6D). Collectively, the overexpression of TRG-AS1 markedly inhibited CRC cells proliferation.

The knockdown of TRG-AS1 in HCT116 and SW480 cells clearly enhanced cell growth as measured by the CCK8 assay, colony formation and EdU (Fig. 7A-C). Overall, these data demonstrated that knockdown TRG-AS1 markedly induced CRC cells proliferation.

3.6 LncRNA TRG-AS1 inhibit cell invasion and migration of CRC cells

Cancer cells use high glycolysis to satisfy the requirement for metastasis [48]. To determine the role of TRG-AS1 in regulating invasion and migration in CRC cells, the ability to invade invasion and migration were examined using Transwell. The results indicated that TRG-AS1 overexpression significantly inhibited invasion and migration. while TRG-AS1 silencing suppressed cell invasion and migration (Fig. 8). These results indicated that silencing of TRG-AS1 promoted cell invasion and migration of colon cancer cells.

4. Discussion

There is a crucial public health concern about the high prevalence of CRC worldwide [49]. Despite extensive study investigating CRC, relatively little is known about the underlying causes and pathogenesis [50, 51]. In the present study, we unveiled a novel lncRNA, TRG-AS1, as a potential biomarker in CRC. To our knowledge, this study first showed an important role of the TRG-AS1 in modulating glucose metabolism in CRC. The expression of TRG-AS1 was considerably reduced in CRC tissues, which suppressed tumor cell glycolysis, proliferation, migration and invasion. To sum up, our pooled results suggested that TRG-AS1 functions as a tumor suppressor in CRC.

Accumulating evidence supports that lncRNAs play critical roles on regulate the expression of genes and involved in the development and progression of cancer through complex tumor networks [52–54]. Cui et al found that LncRNA linc00460 promoted esophageal cancer cell metastatic and epithelial mesenchymal transition process via sponging miR-1224-5p [55].The recently study identified lncRNA RP4-694A7.2 interacted with PSAT1 to promote the proliferation and metastasis of Hepatocellular Carcinoma Cell [56]. To date, studies on the association of TRG-AS1 expression with cancer are limited.

For instance, TRG-AS1 affects cell proliferation and invasion via miR-224-5p/SMAD4 in Lung cancer cells [57]. As a miR-4500 sponge, TRG-AS1 promotes the development of hepatocellular carcinoma [58]. Additionally, TRG-AS1 may act as a pro-oncogenic regulator in tongue squamous cell carcinoma and glioblastoma cell. Interestingly, our study identified TRG-AS1 as a tumor suppressor in colorectal cancer. This disparity may be due to the different conditions of tumor microenvironment, especially the immune cell infiltration and gut microbiota [59]. Inevitably, tumor site and cell line characteristics may also be involved.

Reprogramming of cellular metabolism is currently viewed as a hallmark of cancer, fulfilling the demands of rapid proliferation [60, 61]. For example, lncRNA MIR17HG has been proven to promote CRC liver metastases by mediating a positive feedback loop in the regulation of glycolysis [62]. PTTG3P induction by hypoxia inducible factor-1α targeting the promoter region promoted glycolysis and M2 phenotype of macrophage in CRC [63]. The gut microbiota also seems to be involved. *Fusobacterium nucleatum* promoted CRC glycolysis and tumorigenesis by activating lncRNA ENO1-IT1 transcription [64]. However, the study on lncRNA TRG-AS1 regulated glycolysis in CRC has not been reported previously. We first identified the overexpression of lncRNA TRG-AS1 inhibited glycolysis in CRC cells. Regrettably, the specific molecular mechanisms involved and the verification of animal experiment have not been presented. These problems are the subject of our next research.

5. Conclusions

In general, we demonstrated for the first time that lncRNA TRG-AS1 was lower expression in CRC, and lower lncRNA TRG-AS1 expression levels were association with OS and PFS. At the same time, the biological functions of lncRNA TRG-AS1 in CRC was revealed. This study provided a new perspective to the understanding of the molecular mechanisms in colorectal cancer.

Abbreviations

Abbreviation	Complete
CRC	Colorectal cancer
DEGs	Differentially expressed genes
DFS	Disease Free Survival
GAPDH	Glyceraldehyde 3-phosphate dehydrogenase
GEO	Gene Expression Omnibus
Lnc RNA	Long non-coding RNA
OS	Overall Survival
TCGA	The Cancer Genome Atlas

Declarations

Ethics approval

All experimental procedures have been approved by the Ethics Committee of Zhengzhou Central Hospital Affiliated to Zhengzhou University (Ethical Batch Number:202021).

Consent to participate

Informed consent was obtained from all individual participants included in the study.

Consent for publication

Not applicable

Data Availability Statement

The data that support the findings of this study are available from TCGA and Gene Expression Omnibus (GEO) databases. The public data of TCGA-CRC is available from the TCGA Project (https://xenabrowser.net/datapages).

The public data of GSE15960 (https://www.ncbi.nlm.nih.gov/geo/query/acc.cgi?acc=GSE15960),

GSE9348(https://www.ncbi.nlm.nih.gov/geo/query/acc.cgi?acc=GSE9348),

GSE8671 (https://www.ncbi.nlm.nih.gov/geo/query/acc.cgi?acc=GSE8671),

GSE37364 (https://www.ncbi.nlm.nih.gov/geo/query/acc.cgi?acc=GSE37364),

GSE33133 (https://www.ncbi.nlm.nih.gov/geo/query/acc.cgi?acc=GSE33133),

GSE21510 (https://www.ncbi.nlm.nih.gov/geo/query/acc.cgi?acc=GSE21510)

and GSE39582 (https://www.ncbi.nlm.nih.gov/geo/query/acc.cgi?acc=GSE39582) are available from the GEO database (https://www.ncbi.nlm.nih.gov/geo/).

Conflict ofinterests of statement

The authors have no relevant financial or non-financial interests to disclose.

Funding Sources

This study was supported by the grants from Medical Science and Technology Research Program Joint Project of Henan Province (Grant numbers.LHGJ20210763) and 2021 Cultivation Research Project of Advanced Medical Research Center Branch of Zhengzhou Central Hospital Affiliated to Zhengzhou University (Grant numbers.XJYXZX2021003).

Author Contributions

Lu Li and Yong Zhang performed experiments together. Yong Zhang completed bioinformatics analysis, clinical analysis, and statistical analysis; Lu Li drafted the manuscript; Lu Li and Yong Zhang created figures; Huili Wu and Feifei Chu conceived the project; Mengxuan Xing, Xingguo Xiao, Li Zhang and Kunkun Li contributed to interpretation of the data and revised the manuscript; Kunkun Li, Feifei Chu and Huili Wu directed the research and made the critical revision. All authors identified the manuscript and finally approved the article.

Acknowledgments

The authors gratefully acknowledge the financial supports by Medical Science and Technology Research Program Joint Project of Henan Province (Grant numbers.LHGJ20210763) and 2021 Cultivation Research Project of Advanced Medical Research Center Branch of Zhengzhou Central Hospital Affiliated to Zhengzhou University (Grant numbers.XJYXZX2021003).

We would like to express our sincere thanks to Professor Wei Cao and Dr. Pengju Lv for their experimental technical guidance in this study. We are grateful to Dr. Yuanbo Cui for his valuable suggestions on this study.

References

1. Erratum: Global cancer statistics 2018: GLOBOCAN estimates of incidence and mortality worldwide for 36 cancers in 185 countries. CA Cancer J Clin. 2020;70(4):313. https://doi.org/10.3322/caac.21609.
2. Chandrasekaran B, Pal D, Kolluru V, Tyagi A, Baby B, Dahiya NR, et al. The chemopreventive effect of withaferin A on spontaneous and inflammation-associated colon carcinogenesis models. Carcinogenesis. 2018;39(12):1537–47. https://doi.org/10.1093/carcin/bgy109.
3. Fahmy UA, Aldawsari HM, Badr-Eldin SM, Ahmed O, Alhakamy NA, Alsulimani HH, et al. The Encapsulation of Febuxostat into Emulsomes Strongly Enhances the Cytotoxic Potential of the Drug on HCT 116 Colon Cancer Cells. Pharmaceutics. 2020;12(10). https://doi.org/10.3390/pharmaceutics12100956.
4. Li A, Wang WC, McAlister V, Zhou Q, Zheng X. Circular RNA in colorectal cancer. J Cell Mol Med. 2021;25(8):3667–79. https://doi.org/10.1111/jcmm.16380.
5. Su CM, Weng YS, Kuan LY, Chen JH, Hsu FT. Suppression of PKCδ/NF-κB Signaling and Apoptosis Induction through Extrinsic/Intrinsic Pathways Are Associated Magnolol-Inhibited Tumor Progression in Colorectal Cancer In Vitro and In Vivo. Int J Mol Sci. 2020;21(10). https://doi.org/10.3390/ijms21103527.
6. Burnett-Hartman AN, Lee JK, Demb J, Gupta S. An Update on the Epidemiology, Molecular Characterization, Diagnosis, and Screening Strategies for Early-Onset Colorectal Cancer. Gastroenterology. 2021;160(4):1041–9. https://doi.org/10.1053/j.gastro.2020.12.068.

7. Chen L, He M, Zhang M, Sun Q, Zeng S, Zhao H, et al. The Role of non-coding RNAs in colorectal cancer, with a focus on its autophagy. Pharmacol Ther. 2021;226:107868. https://doi.org/10.1016/j.pharmthera.2021.107868.
8. De Palma F, D'Argenio V, Pol J, Kroemer G, Maiuri MC, Salvatore F. The Molecular Hallmarks of the Serrated Pathway in Colorectal Cancer. Cancers (Basel). 2019;11(7). https://doi.org/10.3390/cancers11071017.
9. Long F, Lin Z, Li L, Ma M, Lu Z, Jing L, et al. Comprehensive landscape and future perspectives of circular RNAs in colorectal cancer. Mol Cancer. 2021;20(1):26. https://doi.org/10.1186/s12943-021-01318-6.
10. Niyaz M, Khan MS, Mudassar S. Hedgehog Signaling: An Achilles' Heel in Cancer. Transl Oncol. 2019;12(10):1334–44. https://doi.org/10.1016/j.tranon.2019.07.004.
11. Dong H, Hu J, Zou K, Ye M, Chen Y, Wu C, et al. Activation of LncRNA TINCR by H3K27 acetylation promotes Trastuzumab resistance and epithelial-mesenchymal transition by targeting MicroRNA-125b in breast Cancer. Mol Cancer. 2019;18(1):3. https://doi.org/10.1186/s12943-018-0931-9.
12. Liang H, Zhao X, Wang C, Sun J, Chen Y, Wang G, et al. Systematic analyses reveal long non-coding RNA (PTAF)-mediated promotion of EMT and invasion-metastasis in serous ovarian cancer. Mol Cancer. 2018;17(1):96. https://doi.org/10.1186/s12943-018-0844-7.
13. Ma M, Xiong W, Hu F, Deng MF, Huang X, Chen JG, et al. A novel pathway regulates social hierarchy via lncRNA AtLAS and postsynaptic synapsin IIb. Cell Res. 2020;30(2):105–18. https://doi.org/10.1038/s41422-020-0273-1.
14. Wang Y, Lu JH, Wu QN, Jin Y, Wang DS, Chen YX, et al. LncRNA LINRIS stabilizes IGF2BP2 and promotes the aerobic glycolysis in colorectal cancer. Mol Cancer. 2019;18(1):174. https://doi.org/10.1186/s12943-019-1105-0.
15. Cui Y, Zhang C, Ma S, Guan F. TFAP2A-induced SLC2A1-AS1 promotes cancer cell proliferation. Biol Chem. 2021;402(6):717–27. https://doi.org/10.1515/hsz-2020-0290.
16. Mohan CD, Rangappa S, Nayak SC, Sethi G, Rangappa KS. Paradoxical functions of long noncoding RNAs in modulating STAT3 signaling pathway in hepatocellular carcinoma. Biochim Biophys Acta Rev Cancer. 2021;1876(1):188574. https://doi.org/10.1016/j.bbcan.2021.188574.
17. Wang Q, He R, Tan T, Li J, Hu Z, Luo W, et al. A novel long non-coding RNA-KAT7 is low expressed in colorectal cancer and acts as a tumor suppressor. Cancer Cell Int. 2019;19:40. https://doi.org/10.1186/s12935-019-0760-y.
18. Wang XD, Lu J, Lin YS, Gao C, Qi F. Functional role of long non-coding RNA CASC19/miR-140-5p/CEMIP axis in colorectal cancer progression in vitro. World J Gastroenterol. 2019;25(14):1697–714. https://doi.org/10.3748/wjg.v25.i14.1697.
19. Zhou M, Guo X, Wang M, Qin R. The patterns of antisense long non-coding RNAs regulating corresponding sense genes in human cancers. J Cancer. 2021;12(5):1499–506. https://doi.org/10.7150/jca.49067.

20. Li Z, Li Y, Wang X, Liang Y, Luo D, Han D, et al. LINC01977 Promotes Breast Cancer Progression and Chemoresistance to Doxorubicin by Targeting miR-212-3p/GOLM1 Axis. Front Oncol. 2021;11:657094. https://doi.org/10.3389/fonc.2021.657094.
21. Ming H, Li B, Zhou L, Goel A, Huang C. Long non-coding RNAs and cancer metastasis: Molecular basis and therapeutic implications. Biochim Biophys Acta Rev Cancer. 2021;1875(2):188519. https://doi.org/10.1016/j.bbcan.2021.188519.
22. Cruickshank BM, Wasson MD, Brown JM, Fernando W, Venkatesh J, Walker OL, et al. LncRNA PART1 Promotes Proliferation and Migration, Is Associated with Cancer Stem Cells, and Alters the miRNA Landscape in Triple-Negative Breast Cancer. Cancers (Basel). 2021;13(11). https://doi.org/10.3390/cancers13112644.
23. Huang PS, Lin YH, Chi HC, Tseng YH, Chen CY, Lin TK, et al. Dysregulated FAM215A Stimulates LAMP2 Expression to Confer Drug-Resistant and Malignant in Human Liver Cancer. Cells. 2020;9(4). https://doi.org/10.3390/cells9040961.
24. Huang QY, Liu GF, Qian XL, Tang LB, Huang QY, Xiong LX. Long Non-Coding RNA: Dual Effects on Breast Cancer Metastasis and Clinical Applications. Cancers (Basel). 2019;11(11). https://doi.org/10.3390/cancers11111802.
25. Nuthikattu S, Milenkovic D, Rutledge JC, Villablanca AC. Lipotoxic Injury Differentially Regulates Brain Microvascular Gene Expression in Male Mice. Nutrients. 2020;12(6). https://doi.org/10.3390/nu12061771.
26. Chou PC, Choi HH, Huang Y, Fuentes-Mattei E, Velazquez-Torres G, Zhang F, et al. Impact of diabetes on promoting the growth of breast cancer. Cancer Commun (Lond). 2021;41(5):414–31. https://doi.org/10.1002/cac2.12147.
27. Soumoy L, Schepkens C, Krayem M, Najem A, Tagliatti V, Ghanem GE, et al. Metabolic Reprogramming in Metastatic Melanoma with Acquired Resistance to Targeted Therapies: Integrative Metabolomic and Proteomic Analysis. Cancers (Basel). 2020;12(5). https://doi.org/10.3390/cancers12051323.
28. Wei J, Huang K, Chen Z, Hu M, Bai Y, Lin S, et al. Characterization of Glycolysis-Associated Molecules in the Tumor Microenvironment Revealed by Pan-Cancer Tissues and Lung Cancer Single Cell Data. Cancers (Basel). 2020;12(7). https://doi.org/10.3390/cancers12071788.
29. Khodabakhsh F, Merikhian P, Eisavand MR, Farahmand L. Crosstalk between MUC1 and VEGF in angiogenesis and metastasis: a review highlighting roles of the MUC1 with an emphasis on metastatic and angiogenic signaling. Cancer Cell Int. 2021;21(1):200. https://doi.org/10.1186/s12935-021-01899-8.
30. Weglarz-Tomczak E, Rijlaarsdam DJ, Tomczak JM, Brul S. GEM-Based Metabolic Profiling for Human Bone Osteosarcoma under Different Glucose and Glutamine Availability. Int J Mol Sci. 2021;22(3). https://doi.org/10.3390/ijms22031470.
31. Guo Y, Lv B, Liu R, Dai Z, Zhang F, Liang Y, et al. Role of LncRNAs in regulating cancer amino acid metabolism. Cancer Cell Int. 2021;21(1):209. https://doi.org/10.1186/s12935-021-01926-8.

32. Xu Y, Qiu M, Shen M, Dong S, Ye G, Shi X, et al. The emerging regulatory roles of long non-coding RNAs implicated in cancer metabolism. Mol Ther. 2021;29(7):2209–18. https://doi.org/10.1016/j.ymthe.2021.03.017.
33. McCarthy DJ, Chen Y, Smyth GK. Differential expression analysis of multifactor RNA-Seq experiments with respect to biological variation. Nucleic Acids Res. 2012;40(10):4288–97. https://doi.org/10.1093/nar/gks042.
34. Ritchie ME, Phipson B, Wu D, Hu Y, Law CW, Shi W, et al. limma powers differential expression analyses for RNA-sequencing and microarray studies. Nucleic Acids Res. 2015;43(7):e47. https://doi.org/10.1093/nar/gkv007.
35. Reimand J, Isserlin R, Voisin V, Kucera M, Tannus-Lopes C, Rostamianfar A, et al. Pathway enrichment analysis and visualization of omics data using g:Profiler, GSEA, Cytoscape and EnrichmentMap. Nat Protoc. 2019;14(2):482–517. https://doi.org/10.1038/s41596-018-0103-9.
36. Brown DA, Himes BT, Kerezoudis P, Chilinda-Salter YM, Grewal SS, Spear JA, et al. Insurance correlates with improved access to care and outcome among glioblastoma patients. Neuro Oncol. 2018;20(10):1374–82. https://doi.org/10.1093/neuonc/noy102.
37. Toubal A, Kiaf B, Beaudoin L, Cagninacci L, Rhimi M, Fruchet B, et al. Mucosal-associated invariant T cells promote inflammation and intestinal dysbiosis leading to metabolic dysfunction during obesity. Nat Commun. 2020;11(1):3755. https://doi.org/10.1038/s41467-020-17307-0.
38. Galamb O, Spisák S, Sipos F, Tóth K, Solymosi N, Wichmann B, et al. Reversal of gene expression changes in the colorectal normal-adenoma pathway by NS398 selective COX2 inhibitor. Br J Cancer. 2010;102(4):765–73. https://doi.org/10.1038/sj.bjc.6605515.
39. Sabates-Bellver J, Van der Flier LG, de Palo M, Cattaneo E, Maake C, Rehrauer H, et al. Transcriptome profile of human colorectal adenomas. Mol Cancer Res. 2007;5(12):1263–75. https://doi.org/10.1158/1541-7786.MCR-07-0267.
40. Hong Y, Downey T, Eu KW, Koh PK, Cheah PY. A 'metastasis-prone' signature for early-stage mismatch-repair proficient sporadic colorectal cancer patients and its implications for possible therapeutics. Clin Exp Metastasis. 2010;27(2):83–90. https://doi.org/10.1007/s10585-010-9305-4.
41. Galamb O, Wichmann B, Sipos F, Spisák S, Krenács T, Tóth K, et al. Dysplasia-carcinoma transition specific transcripts in colonic biopsy samples. PLoS One. 2012;7(11):e48547. https://doi.org/10.1371/journal.pone.0048547.
42. Kemper K, Versloot M, Cameron K, Colak S, de Sousa e Melo F, de Jong JH, et al. Mutations in the Ras-Raf Axis underlie the prognostic value of CD133 in colorectal cancer. Clin Cancer Res. 2012;18(11):3132–41. https://doi.org/10.1158/1078-0432.CCR-11-3066.
43. Marisa L, de Reyniès A, Duval A, Selves J, Gaub MP, Vescovo L, et al. Gene expression classification of colon cancer into molecular subtypes: characterization, validation, and prognostic value. PLoS Med. 2013;10(5):e1001453. https://doi.org/10.1371/journal.pmed.1001453.
44. Tsukamoto S, Ishikawa T, Iida S, Ishiguro M, Mogushi K, Mizushima H, et al. Clinical significance of osteoprotegerin expression in human colorectal cancer. Clin Cancer Res. 2011;17(8):2444–50.

https://doi.org/10.1158/1078-0432.CCR-10-2884.

45. Jorissen RN, Lipton L, Gibbs P, Chapman M, Desai J, Jones IT, et al. DNA copy-number alterations underlie gene expression differences between microsatellite stable and unstable colorectal cancers. Clin Cancer Res. 2008;14(24):8061–9. https://doi.org/10.1158/1078-0432.CCR-08-1431.
46. Xu Y, Wang X, Chu Y, Li J, Wang W, Hu X, et al. Analysis of transcript-wide profile regulated by microsatellite instability of colorectal cancer. Ann Transl Med. 2022;10(4):169. https://doi.org/10.21037/atm-21-6126.
47. Xu R, Wu M, Liu S, Shang W, Li R, Xu J, et al. Glucose metabolism characteristics and TLR8-mediated metabolic control of CD4 + Treg cells in ovarian cancer cells microenvironment. Cell Death Dis. 2021;12(1):22. https://doi.org/10.1038/s41419-020-03272-5.
48. Zheng M, Cao MX, Luo XJ, Li L, Wang K, Wang SS, et al. EZH2 promotes invasion and tumour glycolysis by regulating STAT3 and FoxO1 signalling in human OSCC cells. J Cell Mol Med. 2019;23(10):6942–54. https://doi.org/10.1111/jcmm.14579.
49. Liu F, Ou W, Tang W, Huang Z, Zhu Z, Ding W, et al. Increased AOC1 Expression Promotes Cancer Progression in Colorectal Cancer. Front Oncol. 2021;11:657210. https://doi.org/10.3389/fonc.2021.657210.
50. He JH, Han ZP, Luo JG, Jiang JW, Zhou JB, Chen WM, et al. Hsa_Circ_0007843 Acts as a mIR-518c-5p Sponge to Regulate the Migration and Invasion of Colon Cancer SW480 Cells. Front Genet. 2020;11:9. https://doi.org/10.3389/fgene.2020.00009.
51. Peterova E, Bures J, Moravkova P, Kohoutova D. Tissue mRNA for S100A4, S100A6, S100A8, S100A9, S100A11 and S100P Proteins in Colorectal Neoplasia: A Pilot Study. Molecules. 2021;26(2). https://doi.org/10.3390/molecules26020402.
52. Cao R, Liu S, Zhang J, Ren X, Chen X, Cheng B, et al. Integrative Analysis of TP53INP2 in Head and Neck Squamous Cell Carcinoma. Front Genet. 2021;12:630794. https://doi.org/10.3389/fgene.2021.630794.
53. Lu Y, Guo G, Hong R, Chen X, Sun Y, Liu F, et al. LncRNA HAS2-AS1 Promotes Glioblastoma Proliferation by Sponging miR-137. Front Oncol. 2021;11:634893. https://doi.org/10.3389/fonc.2021.634893.
54. Zhang XW, Li QH, Xu ZD, Dou JJ. STAT1-induced regulation of lncRNA ZFPM2-AS1 predicts poor prognosis and contributes to hepatocellular carcinoma progression via the miR-653/GOLM1 axis. Cell Death Dis. 2021;12(1):31. https://doi.org/10.1038/s41419-020-03300-4.
55. Cui Y, Zhang C, Lian H, Xie L, Xue J, Yin N, et al. LncRNA linc00460 sponges miR-1224-5p to promote esophageal cancer metastatic potential and epithelial-mesenchymal transition. Pathol Res Pract. 2020;216(7):153026. https://doi.org/10.1016/j.prp.2020.153026.
56. Fan Y, Wang L, Ding Y, Sheng Q, Zhang C, Li Y, et al. Long non-coding RNA RP4-694A7.2 Promotes Hepatocellular Carcinoma Cell Proliferation and Metastasis through the Regulation of PSAT1. J Cancer. 2021;12(18):5633–43. https://doi.org/10.7150/jca.59348.

57. Zhang M, Zhu W, Haeryfar M, Jiang S, Jiang X, Chen W, et al. Long Non-Coding RNA TRG-AS1 Promoted Proliferation and Invasion of Lung Cancer Cells Through the miR-224-5p/SMAD4 Axis. Onco Targets Ther. 2021;14:4415–26. https://doi.org/10.2147/OTT.S297336.
58. Sun X, Qian Y, Wang X, Cao R, Zhang J, Chen W, et al. LncRNA TRG-AS1 stimulates hepatocellular carcinoma progression by sponging miR-4500 to modulate BACH1. Cancer Cell Int. 2020;20:367. https://doi.org/10.1186/s12935-020-01440-3.
59. Liu C, Zhou X, Zeng H, Wu D, Liu L. HILPDA Is a Prognostic Biomarker and Correlates With Macrophage Infiltration in Pan-Cancer. Front Oncol. 2021;11:597860. https://doi.org/10.3389/fonc.2021.597860.
60. Al-Koussa H, El Mais N, Maalouf H, Abi-Habib R, El-Sibai M. Arginine deprivation: a potential therapeutic for cancer cell metastasis? A review. Cancer Cell Int. 2020;20:150. https://doi.org/10.1186/s12935-020-01232-9.
61. Wang YQ, Wang HL, Xu J, Tan J, Fu LN, Wang JL, et al. Sirtuin5 contributes to colorectal carcinogenesis by enhancing glutaminolysis in a deglutarylation-dependent manner. Nat Commun. 2018;9(1):545. https://doi.org/10.1038/s41467-018-02951-4.
62. Zhao S, Guan B, Mi Y, Shi D, Wei P, Gu Y, et al. LncRNA MIR17HG promotes colorectal cancer liver metastasis by mediating a glycolysis-associated positive feedback circuit. Oncogene. 2021;40(28):4709–24. https://doi.org/10.1038/s41388-021-01859-6.
63. Wang Y, Yu G, Liu Y, Xie L, Ge J, Zhao G, et al. Hypoxia-induced PTTG3P contributes to colorectal cancer glycolysis and M2 phenotype of macrophage. Biosci Rep. 2021;41(7). https://doi.org/10.1042/BSR20210764.
64. Hong J, Guo F, Lu SY, Shen C, Ma D, Zhang X, et al. F. nucleatum targets lncRNA ENO1-IT1 to promote glycolysis and oncogenesis in colorectal cancer. Gut. 2020. https://doi.org/10.1136/gutjnl-2020-322780.

Figures

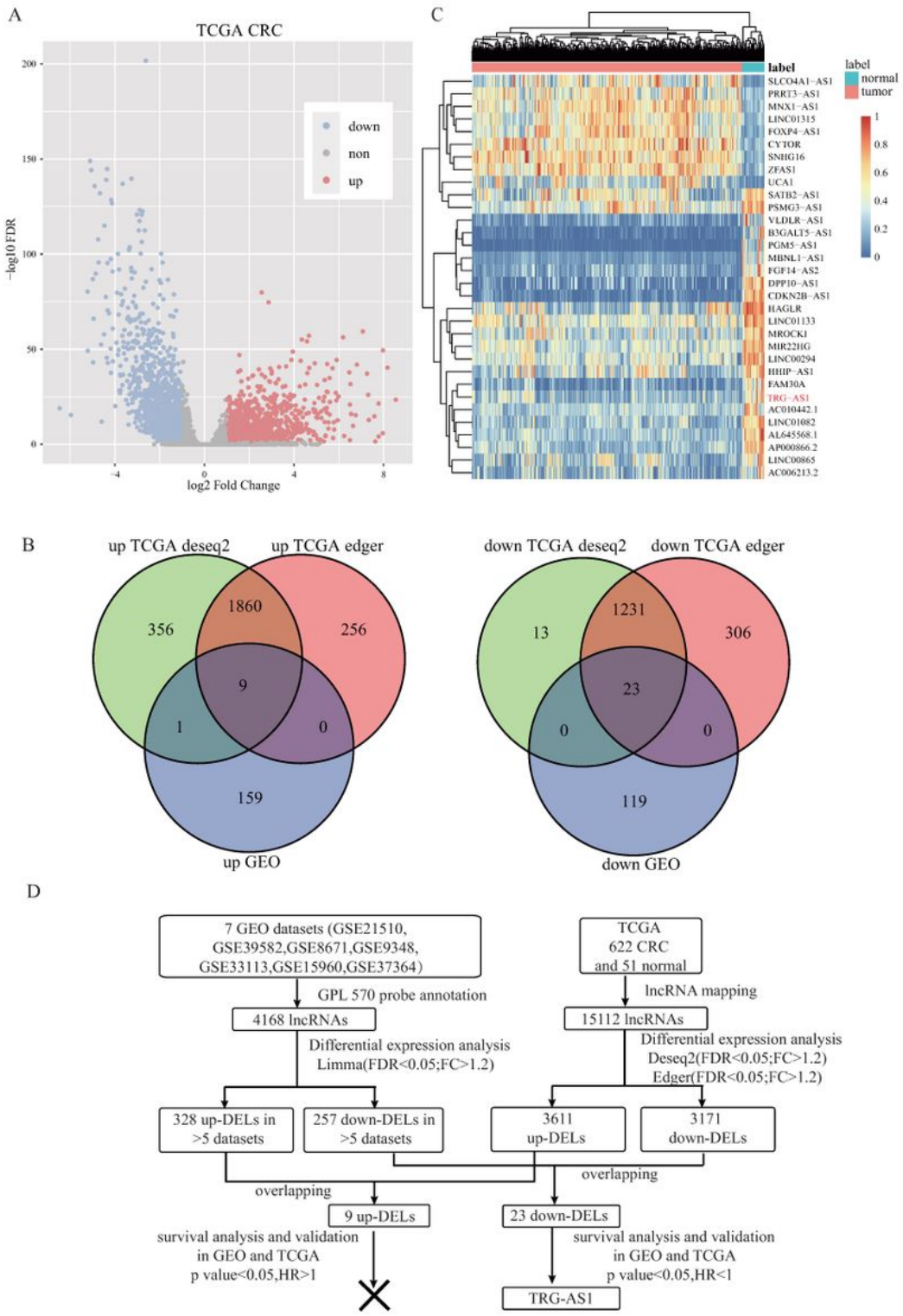

Figure 1

Identification of differentially expressed lncRNAs in colorectal cancer.

(A)Volcano plots of TCGA showing the differentially expressed lncRNAs between CRC samples and normal tissue samples. (B) The overlap between differentially expressed lncRNAs among TCGA and seven GEO databases representation through a Venn diagram. (C) Cluster heat map of differentially

expressed lncRNAs. (D) The Workflow of identification of differentially expressed LncRNAs.(LncRNAs, long non-coding RNAs; TCGA, The Cancer Genome Atlas; CRC, colorectal cancer; GEO, Gene Expression Omnibus)

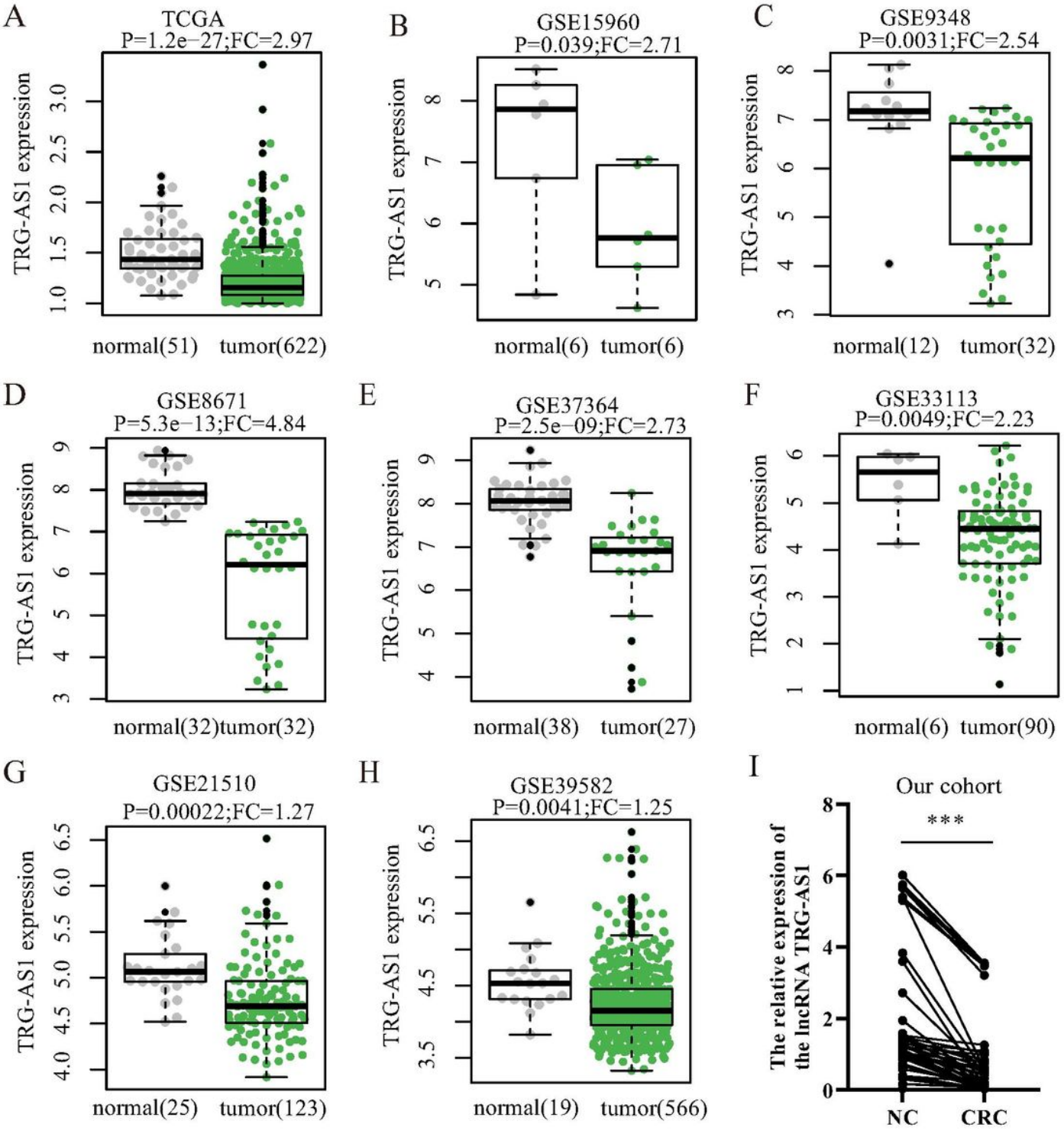

Figure 2

The expression profiles of TRG-AS1.

(A) The relative expression levels of LncRNA TRG-AS1 in normal tissues and colorectal cancer tissues based on TCGA database. (B-H) The relative expression levels of LncRNA TRG-AS1 in normal tissues and colorectal cancer tissues from seven GEO databases. (I) The relative expression levels of LncRNA TRG-AS1 in 66 paired normal tissues and colorectal cancer tissues from our center. (LncRNAs, long non-coding RNAs; TCGA, The Cancer Genome Atlas; CRC, colorectal cancer; GEO, Gene Expression Omnibus; ***$P<0.001$)

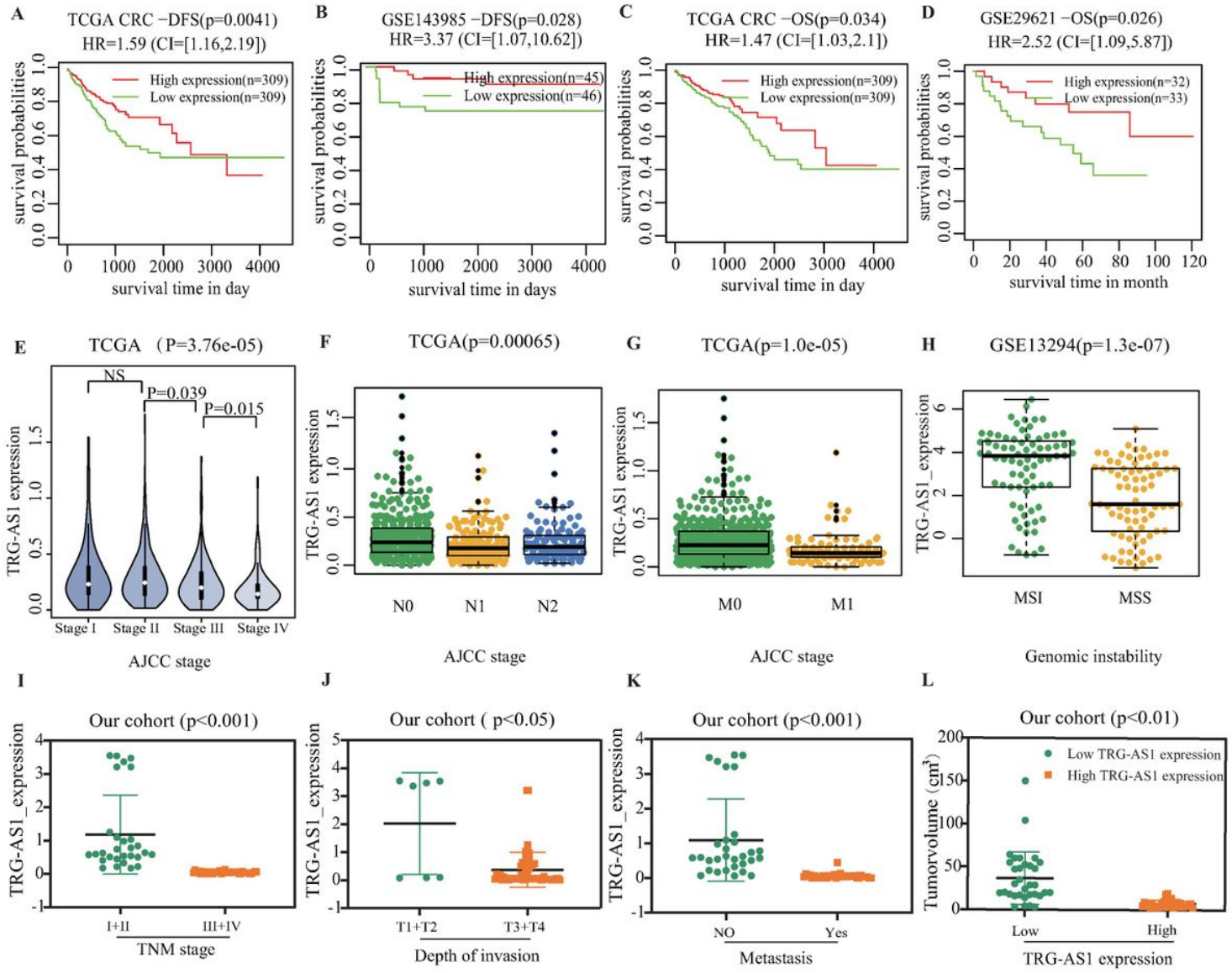

Figure 3

Confirmation of potential prognostic value of TRG-AS1 in CRC.

(A) Kaplan-Meier survival curves for disease-free survival of colorectal cancer patients according to lncRNA TRG-AS1 levels in TCGA database. (B) Kaplan-Meier survival curves for disease-free survival of colorectal cancer patients according to lncRNA TRG-AS1 levels in the GSE143985 database. (C) Kaplan-Meier survival curves for overall survival of colorectal cancer patients according to lncRNA TRG-AS1

levels in TCGA database. (D) Kaplan-Meier survival curves for overall survival of colorectal cancer patients according to lncRNA TRG-AS1 levels in the GSE29621 database. (E) The Correlation between lncRNA TRG-AS1 and AJCC TNM stage in the TCGA database. (F) The Correlation between lncRNA TRG-AS1 and lymph node metastasis in the TCGA database. (G) The Correlation between lncRNA TRG-AS1 and distant metastasis in the TCGA database. (H) The Correlation between lncRNA TRG-AS1 and genomic instability. (I) The correlation of lncRNA TRG-AS1 with TNM stage was analyzed from our cohort. (J) The correlation of lncRNA TRG-AS1 with invasion depth was analyzed from our cohort. (K) The Correlation between lncRNA TRG-AS1 and metastasis in our cohort. (L) The correlation of lncRNA TRG-AS1 with tumor size was analyzed from our center data. (LncRNAs, long non-coding RNAs; TCGA, The Cancer Genome Atlas; CRC, colorectal cancer; GEO, Gene Expression Omnibus)

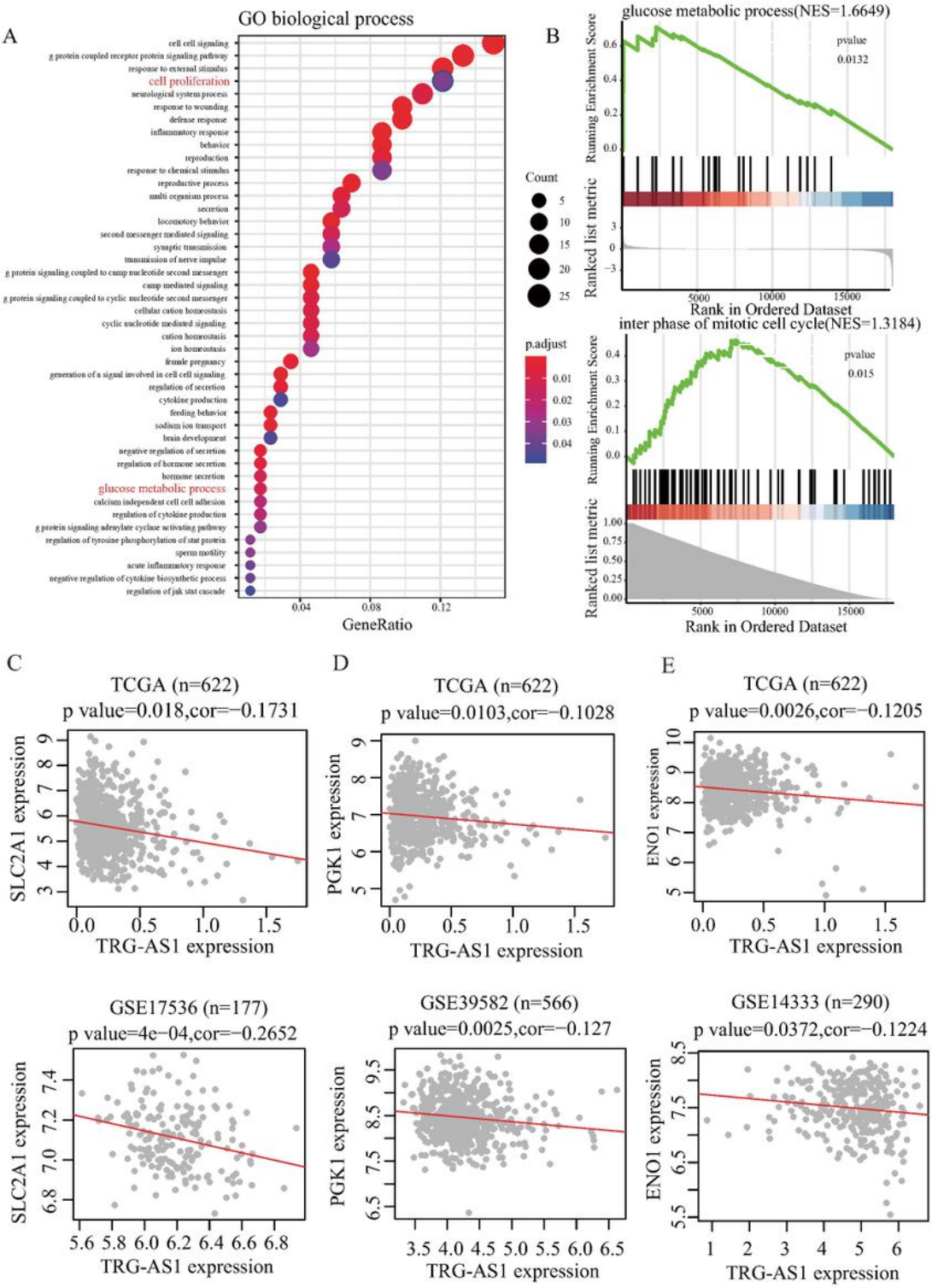

Figure 4

Potential biological functions of TRG-AS1 in CRC

(A-B) Gene Ontology enrichment analyses and GSEA analysis of lncRNA TRG-AS1 were performed. (C-E) The correlations of lncRNA TRG-AS1 with key enzymes of glucose metabolism in public databases were

predicted. (LncRNAs, long non-coding RNAs; TCGA, The Cancer Genome Atlas; GEO, Gene Expression Omnibus)

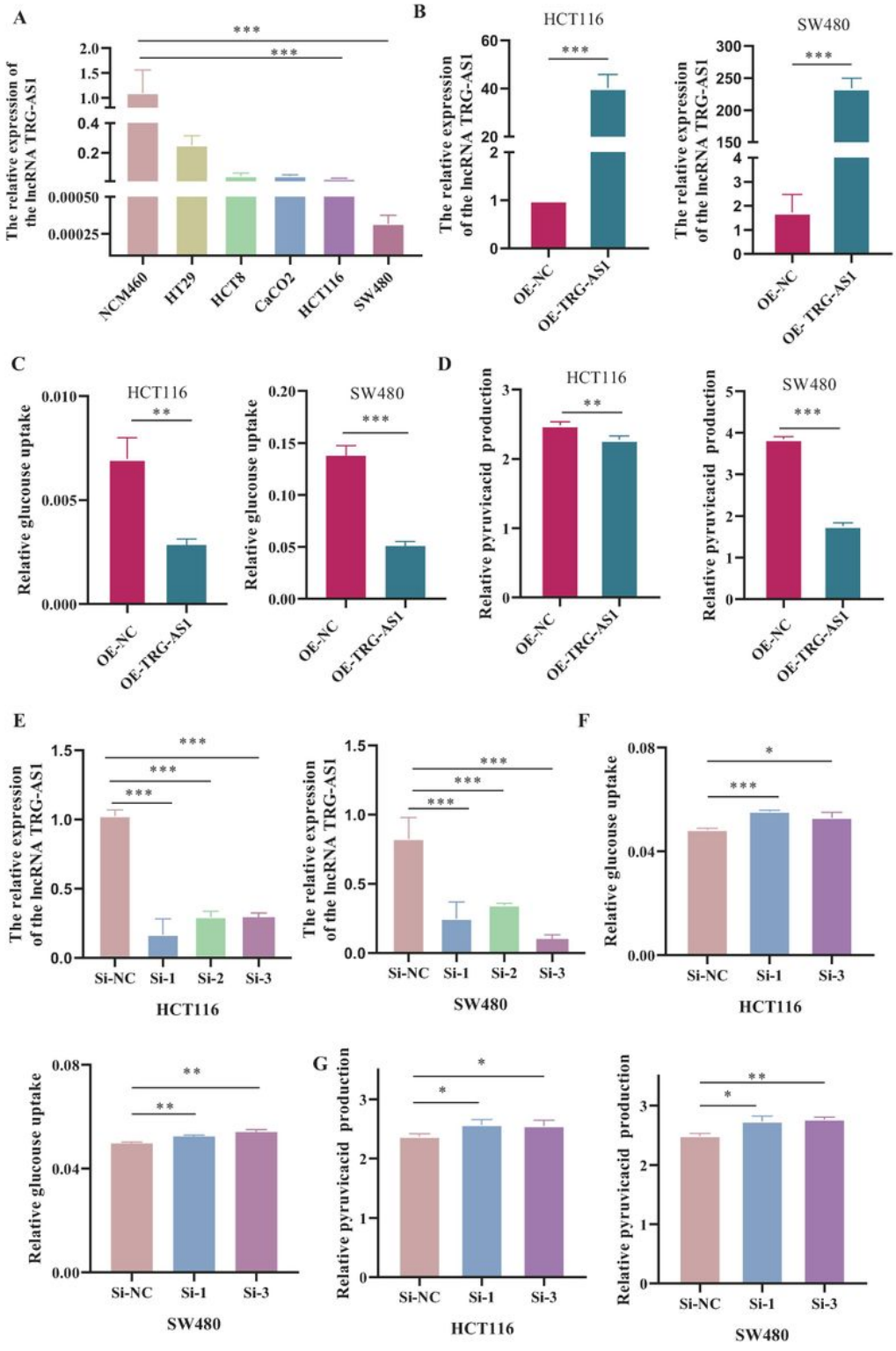

Figure 5

LncRNA TRG-AS1 contributes to weakened glycolysis

(A)The expression levels of lncRNA TRG-AS1 in colon epithelial cells and intestinal cancer cell lines. (B) The overexpression efficiency of lncRNA TRG-AS1 in HCT 116 and SW480 cell lines were detected by q RT-PCR. (C) The glucose uptake capacity was detected in lncRNA TRG-AS1- overexpression HCT 116 and SW480 lines. (D) The relative production of pyruvate in lncRNA-overexpressing HCT 116 and SW480 cell lines. (E) The knockdown efficiency of lncRNA TRG-AS1 in HCT 116 and SW480 cell lines were detected by q RT-PCR. (F) The glucose uptake capacity was detected in lncRNA TRG-AS1-knockdown HCT 116 and SW480 lines. (G) The relative production of pyruvate was detected in lncRNA TRG-AS1-knockdown HCT 116 and SW480 lines. (OE-NC: vector control group, OE-TRG-AS1: lncRNA TRG-AS1 overexpressing groups, T-Si-NC: negative control small interfering RNA, Si-1: target LncRNA TRG-AS1 small interfering RNA 1, Si-3: target LncRNA TRG-AS1 small interfering RNA 3.*, $P<0.05$;**, $P<0.01$;***,$P<0.001$.)

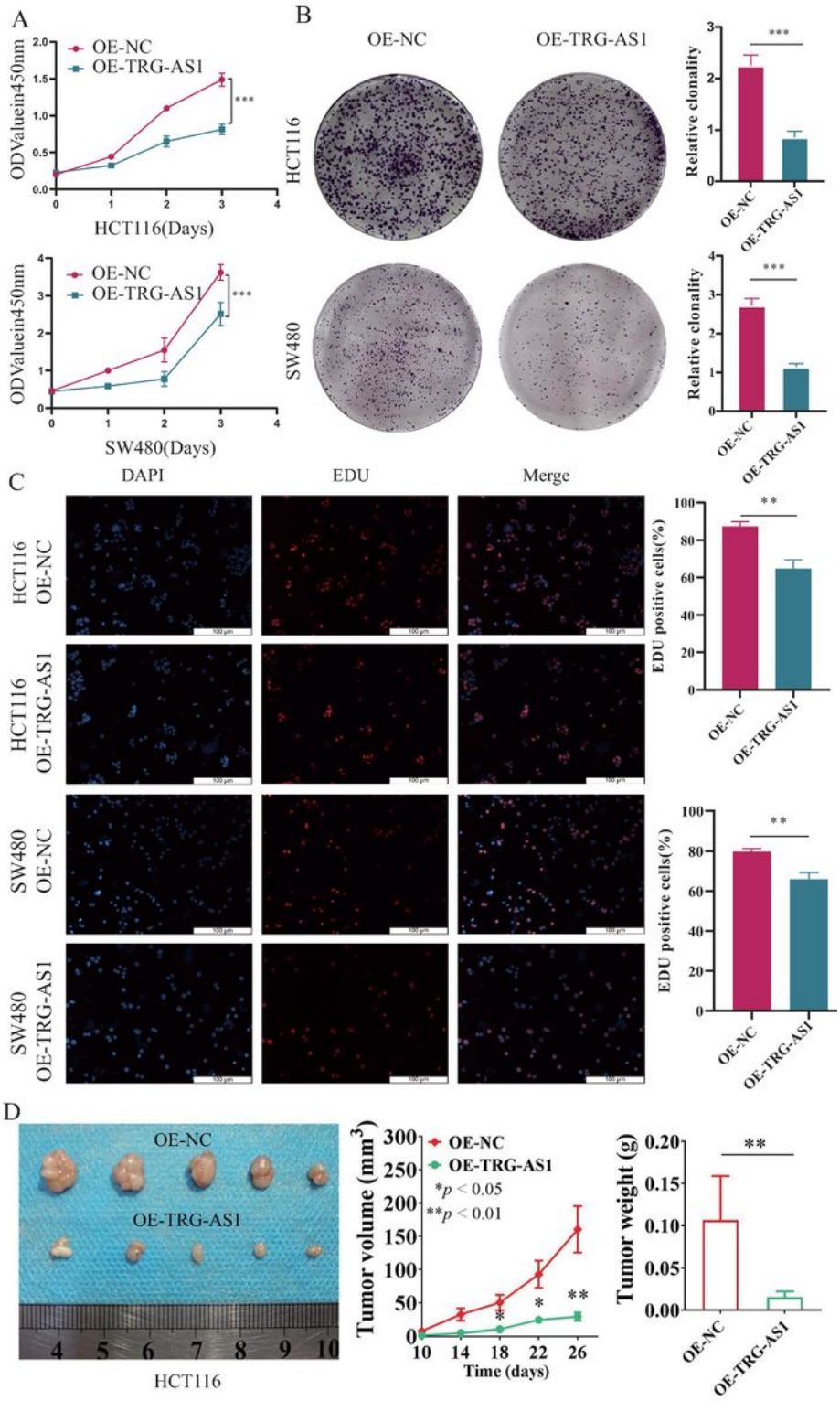

Figure 6

The overexpression of TRG-AS1 inhibits the CRC cell proliferation in vitro and in vivo.

(A) The cell proliferation ability was determined by CCK8 method in vitro. (B) The cell proliferation was measured using plate clone formation in vitro. (C) EDU-incorporating live cells were detected by EDU proliferation assay in vitro. The nucleus was labeled with DAPI (blue). The red colors indicate EDU-

positive nuclei and proliferative cells. (D) LncRNA TRG-AS1 overexpression significantly reduced the volume of tumors by and slowed down the speed of tumor growth in nude mice xenograft tumors. (OE-NC: vector control group, OE-TRG-AS1: lncRNA TRG-AS1 overexpressing groups, * P<0.05, ** P<0.01, *** P<0.001)

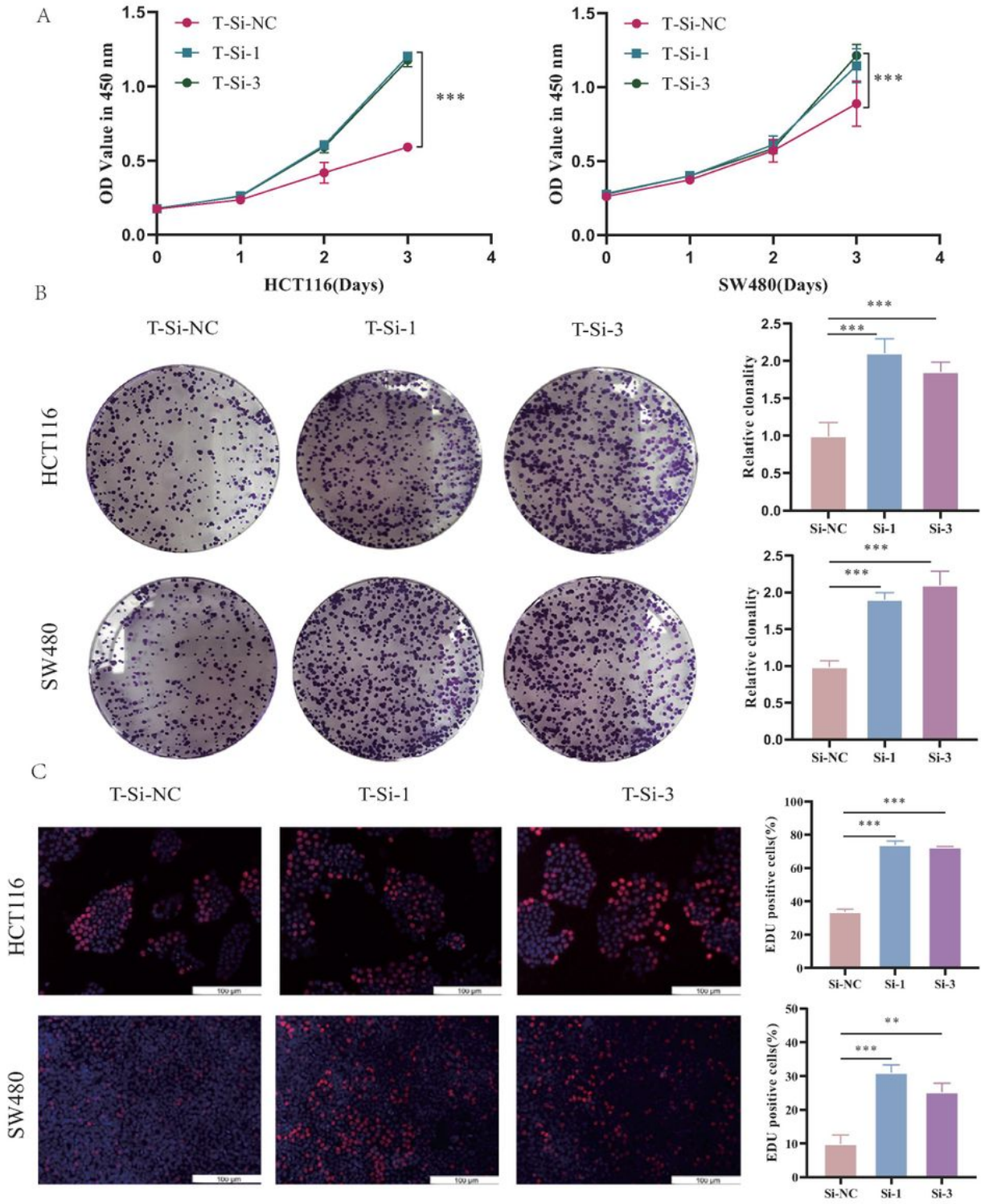

Figure 7

The knockdown of lncRNA TRG-AS1 promotes the colorectal cancer cell proliferation.

(A) The cell proliferation ability was determined by CCK8 method. (B) The cell proliferation was measured using plate clone formation. (C) EDU-incorporating live cells were detected by EDU proliferation assay. The nucleus was labeled with DAPI (blue). The red colors indicate EDU-positive nuclei and proliferative cells. (T-Si-1: target LncRNA TRG-AS1 small interfering RNA 1, T-Si-3: target LncRNA TRG-AS1 small interfering RNA 3. ***P<0.001)

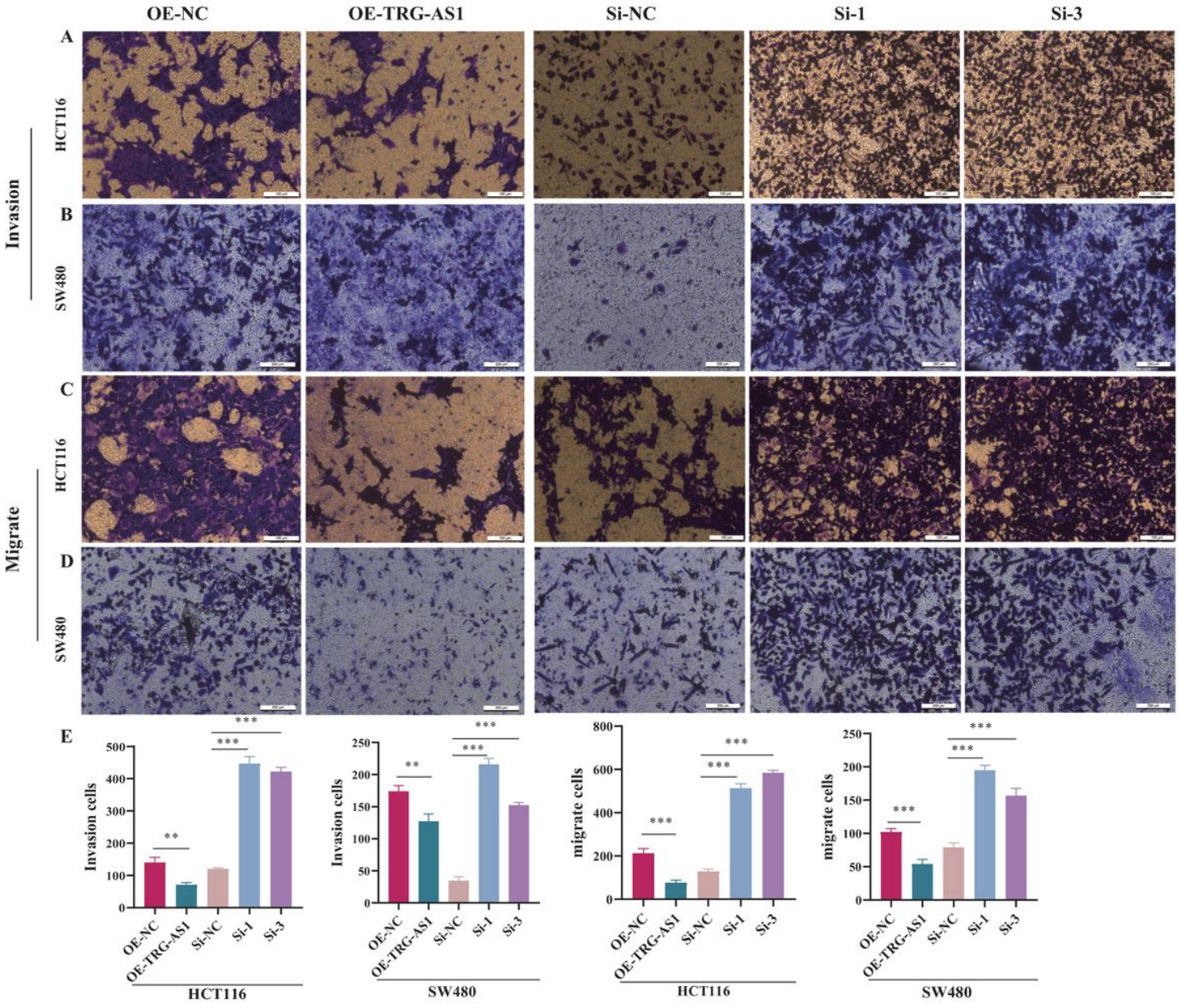

Figure 8

LncRNA TRG-AS1 inhibits the metastatic potential of CRC cells.

(A) Transwell assay was performed to detect the invasive abilities of HCT116 cell after LncRNA TRG-AS1 overexpression or knockdown. (B) Transwell assay was performed to detect the invasive abilities of

SW480 cell after LncRNA TRG-AS1 overexpression or knockdown. (C) Transwell assay was performed to detect the migratory abilities of HCT116 cell after LncRNA TRG-AS1 overexpression or knockdown. (D) Transwell assay was performed to detect the migratory abilities of SW480 cell after LncRNA TRG-AS1 overexpression or knockdown. (E) The numbers of cells that migrated and invaded were quantified. (OE-NC: vector control group, OE-TRG-AS1: lncRNA TRG-AS1 overexpressing groups, Si-NC: negative control small interfering RNA, Si-1: target LncRNA TRG-AS1 small interfering RNA 1, Si-3: target LncRNA TRG-AS1 small interfering RNA 3)